Brandenburg, A., Nordlund, Å., Pulkkinen, P., Stein, R.F., Tuominen, I.: 1990, "Turbulent diffusivities derived from simulations," in *Proceedings of the Finnish Astronomical Society 1990*, eds. K. Muinonen, M. Kokko, S. Pohjolainen, and P. Hakala, Helsinki 1990, p. 1-4

Turbulent diffusivities derived from simulations

A. Brandenburg[1], Å. Nordlund[2], P. Pulkkinen[3], R. F. Stein[4], and I. Tuominen[1]

[1] Observatory and Astrophysics Laboratory, University of Helsinki, Tähtitorninmäki, SF-00130 Helsinki, Finland
[2] Copenhagen University Observatory, Øster Voldgade 3, DK-1350 Copenhagen K, Denmark
[3] Department of Theoretical Physics, University of Helsinki, Siltavuorenpenger 20 C, SF-00170 Helsinki, Finland
[4] Department of Physics and Astronomy, Michigan State University, East Lancing, Michigan 48824-1116, USA

Abstract. By employing direct simulations of turbulent magneto-convection we determine the turbulent diffusivities, such as the turbulent magnetic diffusivity, the eddy viscosity and the turbulent heat conductivity. The fluid extends over one scale height and is confined between impenetrable boundaries. With our technique it is essential for the determination of such quantities to enforce a non-vanishing mean current and a gradient in the mean velocity. We find that the order of magnitude obtained for the various turbulent diffusivities is in some cases compatible with the customary expression $\frac{1}{3}u_t\ell$, where u_t is the rms-velocity and $\ell = d$ is the mixing length which is here taken to be the depth of the layer. However, there is evidence that the eddy viscosity does not allow a suitable description in the present cases where the turbulence is caused by convection. Finally, results for the mean Lorentz force are presented and discussed in the context of recent predictions based on the first order smoothing approach.

Key words: stellar convection – turbulence – turbulent diffusion – mean-field dynamo – the Sun: magnetic fields

1. Introduction

In a previous paper (Brandenburg et al., 1990, hereafter referred to as Paper I) we have described a method for determining mean-field transport coefficients, such as the α-effect and the turbulent magnetic diffusivity, by means of direct simulations of turbulent magneto-convection. These turbulent transport coefficients describe the dependence of certain correlation functions on the mean magnetic field $\langle \boldsymbol{B} \rangle$, the mean velocity $\langle \boldsymbol{u} \rangle$, and other quantities. They allow closure of the differential equations for $\langle \boldsymbol{u} \rangle$, $\langle \boldsymbol{B} \rangle$, and other (thermodynamic) quantities. Such equations are employed for example in mean-field dynamo theory (e.g. Krause & Rädler, 1980).

In Paper I we chose boundary and initial conditions such that a systematic average magnetic field with a certain orientation is present. By "systematic" we mean a mean field whose properties are independent of details of the initial conditions, so that its spatial variation and magnitude are then more-or-less predictable. This approach reflects the intention of simulating the turbulent flow only in a small *test volume* in the solar convection zone.

Our previous results have indicated the importance of anisotropies in the α-effect. The determination of the turbulent magnetic diffusivity η_t, however, seemed somewhat unreliable because negative values were typically obtained. This is unphysical, because the mean-field equations possess stable solutions only for positive turbulent diffusivities.

One of the aims of this paper is to reconsider the determination of η_t. In the theory of mean-field electrodynamics it is shown that the turbulent electromotive force $\langle \boldsymbol{u}' \times \boldsymbol{B}' \rangle$ can be expressed as a linear functional of $\langle \boldsymbol{B} \rangle$. For example in the simplest case of isotropic turbulence one finds

$$\langle \boldsymbol{u}' \times \boldsymbol{B}' \rangle = \alpha \langle \boldsymbol{B} \rangle - \eta_t \mathrm{curl} \langle \boldsymbol{B} \rangle$$

(e.g. Roberts & Sowards, 1975). In the models investigated in Paper I the x- and y-components were equally preferred. Typically, the horizontal components of $\mathrm{curl} \langle \boldsymbol{B} \rangle$ are then nearly vanishing and the vertical component of $\mathrm{curl} \langle \boldsymbol{B} \rangle$ vanishes identically since $\mathrm{div} \langle \boldsymbol{B} \rangle = 0$ and by definition of the averages adopted (cf. Paper I). Thus, η_t multiplies a very small quantity. This makes an reliable determination of η_t impossible. It appears therefore necessary to impose a systematic (vertical) gradient in $\langle \boldsymbol{B} \rangle$. This can be done by choosing appropriate boundary conditions. The same concept can be applied to the determination of ν_t by imposing a systematic vertical gradient in the average velocity $\langle \boldsymbol{u} \rangle$.

This paper is organized as follows. In Sect. 2 we summarize the basic equations and describe briefly the model for simulating magneto-convection. The equations for determining α and η_t are given in Sect. 3. Results for η_t and also for the eddy viscosity and the turbulent heat conductivity are shown in Sect. 4. Finally, we discuss implications for the mean Lorentz force (Sect. 5) and give our conclusions (Sect. 6).

2. Simulating magneto-convection

We consider a fully compressible fluid heated from below and take the dynamical effects of magnetic fields and rotation into account. We are interested in the lower layers of the convection zone and can treat radiation therefore in the diffusion approximation. We assume all variables to be periodic in the horizontal direction. This is numerically convenient and avoids artificial boundaries. (However, it is then impossible to include the centrifugal force in the momentum equation; see discussion in Paper I.)

We solve the equations for conservation of mass, momentum, energy, and the induction equation in the form

$$\frac{\mathrm{D}\ln\rho}{\mathrm{D}t} + \mathrm{div}\,\boldsymbol{u} = 0, \tag{1}$$

$$\frac{\mathrm{D}\boldsymbol{u}}{\mathrm{D}t} = -\frac{p}{\rho}\nabla\ln p + \boldsymbol{g} - 2\boldsymbol{\Omega}\times\boldsymbol{u} + \frac{1}{\rho}\boldsymbol{J}\times\boldsymbol{B} + \frac{\mu}{\rho}(\nabla^2\boldsymbol{u} + \tfrac{1}{3}\nabla\nabla\cdot\boldsymbol{u}), \tag{2}$$

$$\frac{\mathrm{D}e}{\mathrm{D}t} = -\frac{p}{\rho}\,\mathrm{div}\,\boldsymbol{u} + \frac{\mathcal{K}}{\rho}\nabla^2 e + Q_{\rm visc} + Q_{\rm Joule}, \tag{3}$$

$$\frac{\partial\boldsymbol{B}}{\partial t} = \mathrm{curl}\,(\boldsymbol{u}\times\boldsymbol{B} - \boldsymbol{J}/\sigma), \tag{4}$$

where e is the specific internal energy of the gas which we assume to be ideal, i.e. $p/\rho = (\gamma-1)e$. Here, γ is the ratio of the specific heats c_p and c_v, which are assumed to be constant. $Q_{\rm visc}$ is the rate of viscous heating, and $Q_{\rm Joule} = \boldsymbol{J}^2/\rho\sigma$ is the rate of Joule heating per unit mass, $\boldsymbol{J} = \mathrm{curl}\,\boldsymbol{B}/\mu_0$ is the electric current, and σ the electric conductivity. If the condition $\mathrm{div}\,\boldsymbol{B} = 0$ is satisfied by the initial field, $\mathrm{div}\,\boldsymbol{B}$ remains zero. In the derivation of Eqs. (2) and (3) we have assumed constant values for μ and $\mathcal{K}$.

As in Paper I we exclude penetration of the motions through the boundaries of the computational volume. If not stated otherwise we require the horizontal components of viscous and magnetic stress to vanish on both boundaries, i.e. $u_{1,3} = u_{2,3} = u_3 = 0$ and $B_1 = B_2 = 0$ at the top and bottom. Commas denote derivatives and index 3 refers to the z-direction. We keep e constant at the top and prescribe the vertical gradient of e on the bottom.

The initial velocity field consists of a superposition of many, spatially smooth, but randomly distributed perturbations in all three components. We take the ratio between horizontal and vertical extent of the model (aspect ratio) $A = 2$, a density contrast $\chi = 2$, and $\gamma = 5/3$. The Chandrasekhar number is $Q = B_0^2 d^2/\mu_0\mu\eta = 72$, and the Taylor number is $\mathrm{Ta} = 10^4$. The two Prandtl numbers, Pr and $\mathrm{P_m}$, are taken to be unity. Non-dimensional quantities are introduced by measuring time in sound travel times (see Paper I). The unit length is the depth of the layer. Density is measured in units of the inital density at the top, ρ_0.

We solve the equations (1)-(4) numerically, using a modification of the code by Nordlund and Stein (1989), that employs a second order Adams-Bashforth time advance and spatial derivatives calculated from cubic splines. Further details were described in Paper I. The calculations were carried out on the Cray XMP-EA/432 of the National Computing Center of Finland. For a resolution of 31^3 meshpoints the code needs about 0.1-0.2 sec real time per time step and 1.3 Mwords of memory. A typical run covering one diffusion time (500 sound travel times) requires 10^5 timesteps.

3. Determining transport coefficients from simulations

We split the velocity and the magnetic field into mean and fluctuating parts, i.e. $\boldsymbol{u} = \langle\boldsymbol{u}\rangle + \boldsymbol{u}'$ and $\boldsymbol{B} = \langle\boldsymbol{B}\rangle + \boldsymbol{B}'$. We adopt here a combined horizontal and temporal average, i.e. $\langle f\rangle = \int dt\,dx\,dy\,f / \int dt\,dx\,dy$. Averaging the induction equation (4) leads to a new term

$$\mathcal{E} = \langle\boldsymbol{u}'\times\boldsymbol{B}'\rangle. \tag{5}$$

In the theory of mean-field electrodynamics $\mathcal{E}$ is expressed as a linear functional of $\langle\boldsymbol{B}\rangle$ with

$$\mathcal{E}_i = \alpha_{ij}\langle\boldsymbol{B}_j\rangle - \beta_{ijk}\partial_k\langle\boldsymbol{B}_j\rangle. \tag{6}$$

(e.g. Krause & Rädler, 1980). In Paper I we concentrated primarily on the determination of α_{ij}. The basic result was that only an anisotropic α-tensor can explain the numerically determined dependence $\mathcal{E} = \mathcal{E}(\boldsymbol{B})$. Writing $\alpha_{ij} = \alpha_1\delta_{ij} + \alpha_2\hat{g}_i\hat{g}_j$ it turned out that α_1 and $\alpha_1 + \alpha_2$ have opposite signs. Here, $\hat{\boldsymbol{g}}$ is the unit vector in the direction of gravity.

In the following we wish to determine the β-tensor. The simplest possible form for β_{ijk} is proportional to the totally antisymmetric tensor ϵ_{ijk}. Writing $\beta_{ijk} = \eta_t\epsilon_{ijk}$ we have then

$$\mathcal{E} = \alpha_H\langle\boldsymbol{B}_H\rangle + \alpha_V\langle\boldsymbol{B}_V\rangle - \eta_t\mu_0\langle\boldsymbol{J}\rangle, \tag{7}$$

where $\langle\boldsymbol{B}_H\rangle = \hat{\boldsymbol{x}}\langle B_x\rangle + \hat{\boldsymbol{y}}\langle B_y\rangle$, $\langle\boldsymbol{B}_V\rangle = \hat{\boldsymbol{z}}\langle B_z\rangle$, and $\mu_0\langle\boldsymbol{J}\rangle = \mathrm{curl}\,\langle\boldsymbol{B}\rangle$. α_H, α_V, and η_t can be readily determined from this equation by multiplying with $\langle\boldsymbol{B}_V\rangle$, $\langle\boldsymbol{B}_H\rangle$, and $\langle\boldsymbol{J}\rangle$. Note that $\langle J_z\rangle = 0$ by definition of the horizontal averages adopted. We then find

$$\alpha_V = \mathcal{E}_z/\langle B_z\rangle, \tag{8}$$

$$\alpha_H = \frac{(\mathcal{E}\cdot\langle\boldsymbol{B}_H\rangle)\langle\boldsymbol{J}\rangle^2 - (\mathcal{E}\cdot\langle\boldsymbol{J}\rangle)(\langle\boldsymbol{J}\rangle\cdot\langle\boldsymbol{B}_H\rangle)}{\langle\boldsymbol{B}_H\rangle^2\langle\boldsymbol{J}\rangle^2 - (\langle\boldsymbol{J}\rangle\cdot\langle\boldsymbol{B}_H\rangle)^2}, \tag{9}$$

$$\eta_t\mu_0 = -\frac{(\mathcal{E}\cdot\langle\boldsymbol{J}\rangle)\langle\boldsymbol{B}_H\rangle^2 - (\mathcal{E}\cdot\langle\boldsymbol{B}_H\rangle)(\langle\boldsymbol{J}\rangle\cdot\langle\boldsymbol{B}_H\rangle)}{\langle\boldsymbol{B}_H\rangle^2\langle\boldsymbol{J}\rangle^2 - (\langle\boldsymbol{J}\rangle\cdot\langle\boldsymbol{B}_H\rangle)^2}. \tag{10}$$

Although we have always used the above expressions, it is worthwhile to note for the purpose of discussion that a good approximation is usually $\alpha_H = \mathcal{E}\cdot\langle\boldsymbol{B}_H\rangle/\langle\boldsymbol{B}_H\rangle^2$ and $\eta_t\mu_0 = -\mathcal{E}\cdot\langle\boldsymbol{J}\rangle/\langle\boldsymbol{J}\rangle^2$.

4. Turbulent diffusivities

4.1. The turbulent magnetic diffusivity

As discussed in the Introduction we impose here a gradient of the y-component of $\langle\boldsymbol{B}\rangle$ by replacing the boundary condition $B_2 = 0$ at top *and* bottom by

$$\begin{aligned} B_2 &= 0 \quad \text{at the top,} \\ B_2 &= B_0 \quad \text{at the bottom.} \end{aligned} \tag{11}$$

This leads to a systematic electric current in the x-direction. The resulting depth dependence of η_t is displayed in the lower panel of Fig. 1. The corresponding profile of α_H, derived from Eq. (9), is shown in the upper panel. The results for α_H and η_t are more-or-less independent of the magnetic field strength (cf. dotted and solid lines in Fig. 1). This means that a *linear* functional dependence $\mathcal{E} = \mathcal{E}(\boldsymbol{B})$ is in principle justified. The

resulting turbulent magnetic diffusivity, derived from Eq. (10), has then a *positive* extremum in the middle of the layer with $\max(\eta_t) \approx 5\eta$. This value seems to be very small. This is a consequence of the small Reynolds number $\mathrm{Re} = u_t d/\nu$ which is in the present case approximately 25. (Much higher values are normally not accessible with only 31 meshpoints in one direction.) The customary expression for the turbulent diffusivity is $\frac{1}{3}u_t\ell$, where u_t is the rms-velocity. Assuming the mixing length to be the depth of the layer ($\ell = d$) we find here $\eta_t \approx 0.2 u_t \ell$.

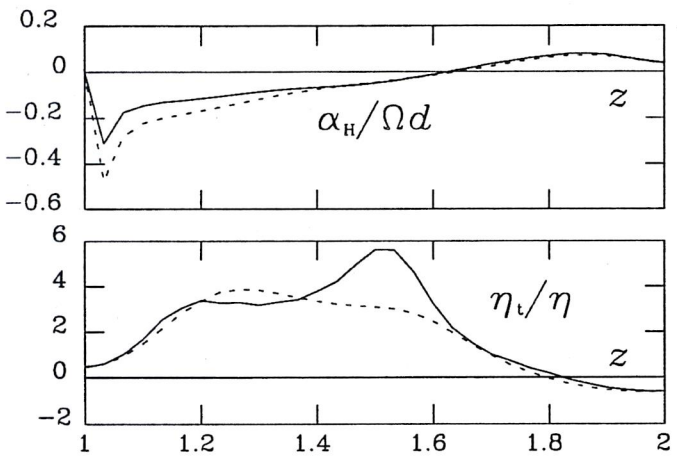

Fig. 1. The profiles of α_H (normalized with Ωd, upper panel) and η_t (normalized with η, lower panel) for $Q = 72$. The dotted curves refer to a run with $Q = 31$

4.2. Eddy viscosity?

It is tempting to determine the eddy viscosity ν_t similarily by imposing a systematic gradient in $\langle \boldsymbol{u} \rangle$. The usual Boussinesq ansatz for the Reynolds stress is

$$\langle u_i' u_j' \rangle = -\nu_t(\langle u_{i,j} \rangle + \langle u_{j,i} \rangle) - \mu_t \delta_{ij} \mathrm{div}\, \langle \boldsymbol{u} \rangle. \qquad (12)$$

Further (non-diffusive) terms enter into Eq. (12) due to the presence of rotation. In the compressible case further terms occur. However, in the cases considered below we find always $\langle \rho' u_i' \rangle \ll \langle \rho \rangle \langle u_i \rangle$.

A systematic gradient in the velocity can be achieved by replacing the boundary condition $u_{2,3} = 0$ by

$$u_{2,3} = U_{23} \quad \text{at top and bottom,} \qquad (13)$$

where U_{23} is some constant. This boundary condition is a generalization of the stress free condition $u_{2,3} = 0$, which is in contrast to a rigid one where u_2 is prescribed.

We have computed models for different values of U_{23}. The resulting profiles of $\langle u_2' u_3' \rangle$ and $\langle u_{2,3} \rangle$ are shown in Fig. 2. Note that $\langle u_2' u_3' \rangle$ is always negative. This means that vertical transport of momentum ρu_2 is upwards, i.e. in the negative z-direction. In the upper parts u_2 is smaller than in the lower parts. Downflow transports a deficit velocity into regions with larger u_2 and vice versa. It is remarkable that the gradient $\langle u_{2,3} \rangle$, imposed at both boundaries, becomes very small in the inner parts of the layer. In fact, $\langle u_{2,3} \rangle$ does even change sign. This means that in this case the vertical transport of momentum cannot be described by positive eddy viscosity coefficients. In other words, the simple expression (12) is *not* suitable to describe the Reynolds stress $\langle u_2' u_3' \rangle$ by means of gradients of the average velocity $\langle u_2 \rangle$.

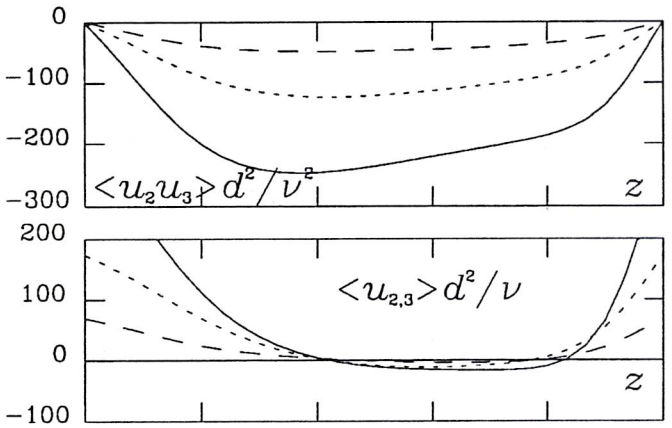

Fig. 2. The profiles of $u_2 u_3$ and $u_{2,3}$ (normalized with d^2/ν^2 and d^2/ν, respectively). The solid lines are for $U_{23} = 1.0$. The dotted and dashed curves refer to runs with $U_{23} = 0.5$ and 0.2, respectively

4.3. Turbulent heat conductivity

Let us finally consider the turbulent heat conductivity χ_t. In a compressible stratified medium the convective flux $\boldsymbol{F}_{\mathrm{conv}} = \gamma \langle e \rho \boldsymbol{u} \rangle$ scales with the entropy gradient, $\nabla \langle s \rangle$, via

$$\boldsymbol{F}_{\mathrm{conv}} = -\chi_t \langle \gamma e \rangle \langle \rho \rangle \nabla \langle s/c_p \rangle. \qquad (14)$$

The resulting profile for χ_t is displayed in the lower panel of Fig. 3. In the upper panel are also shown the z-components of $\boldsymbol{F}_{\mathrm{conv}}$ and $\boldsymbol{F}_{\mathrm{rad}}$.

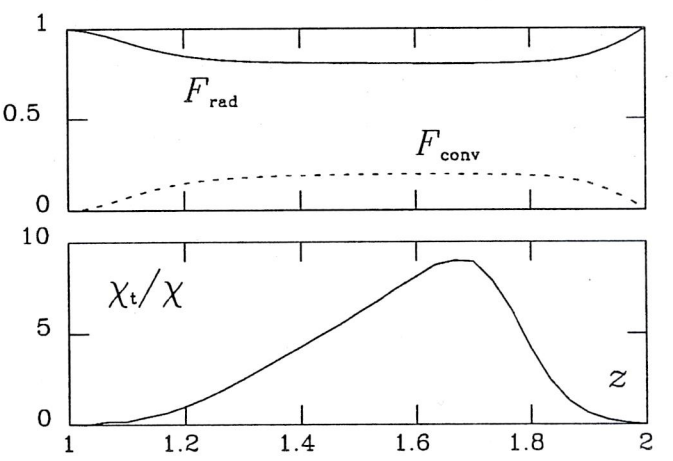

Fig. 3. The profiles for χ_t normalized with $\chi = \mathcal{K}/\rho_0$ (lower panel) and the z-components of $\boldsymbol{F}_{\mathrm{conv}}$ and $\boldsymbol{F}_{\mathrm{rad}}$ normalized with the total flux (upper panel)

5. The mean Lorentz force

The presence of a systematic mean current $\langle \boldsymbol{J} \rangle$ in the simulations allows us to investigate also the mean Lorentz force $\langle \boldsymbol{J} \times \boldsymbol{B} \rangle$. This quantity has been investigated recently by Rüdiger & Kichatinov (1990). They have stressed that for a wide class of turbulence models it is possible for $\langle \boldsymbol{J} \times \boldsymbol{B} \rangle$ to degenerate to a gradient term. This would have dramatic consequences for the theory of the solar torsional oscillations. Note however that this result is obtained in the framework of the first order smoothing approximation. The result for $\langle B_i' B_j' \rangle$ derived by Rüdiger & Kichatinov is similar to that found by Roberts & Sowards (1975) and it leads to

$$\langle \boldsymbol{J} \times \boldsymbol{B} \rangle = -(\frac{\eta_t}{\eta} - 1)\langle \boldsymbol{J} \rangle \times \langle \boldsymbol{B} \rangle - \frac{\eta_t}{\eta} \nabla \langle \boldsymbol{B} \rangle^2 / \mu_0. \qquad (15)$$

In Fig. 4 we present the result for $\langle \boldsymbol{J} \times \boldsymbol{B} \rangle$ obtained from our simulations taking Eq. (11) as boundary condition. Additionally we take $B_3 = B_0$ as initial condition. This leads to a constant $\langle B_3 \rangle$, following from div $\langle \boldsymbol{B} \rangle = 0$ and the assumption of periodic boundary conditions in the horizontal direction (Paper I). The systematic Lorentz force is expected to be $\langle \boldsymbol{J} \rangle \times \langle \boldsymbol{B} \rangle \approx (0, d, d - z) B_0^2 / \mu_0 d^2$.

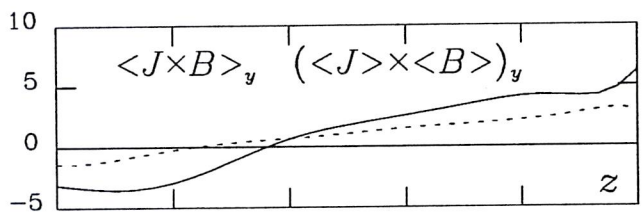

Fig. 4. The y-component of $\langle \boldsymbol{J} \times \boldsymbol{B} \rangle$ (solid lines) compared with $\langle \boldsymbol{J} \rangle \times \langle \boldsymbol{B} \rangle$ (dotted lines). The curves are in units of $B_0^2/\mu_0 d$

The result for the y-component of $\langle \boldsymbol{J} \times \boldsymbol{B} \rangle$ is shown in Fig. 4. We see that $\langle \boldsymbol{J} \times \boldsymbol{B} \rangle_y$ is twice as large as $(\langle \boldsymbol{J} \rangle \times \langle \boldsymbol{B} \rangle)_y$. This is in contrast to Eq. (15), which would predict the opposite behavior.

One should bear in mind that the results presented here cannot be compared directly with those obtained in the framework of first order smoothing. Both approaches represent two extreme cases: here we deal with relatively slow and smooth flows confined in a thin layer whereas first order smoothing is applicable only to flows with short correlation time and short correlation length. Our results should therefore merely be understood just as a demonstration of the other extreme.

6. Discussion

The present investigations have shown that convective turbulence can efficiently smooth advected quantities ($\boldsymbol{B}$, $\boldsymbol{u}$, and s) in the vertical direction. The approach to describe this by z-dependent diffusivities may be in some cases questionable. This becomes evident in particular when the vertical gradients of these quantities change sign. It is also questionable, whether the retained z-dependence of the averages is useful. The correlation length in the z-direction is in our model already comparable with the height of the box. Alternatively one could therefore average also over the z-direction

This result that advected quantities are efficiently smoothed out in the vertical direction may have implications for understanding properties of the solar differential rotation. The dominant feature of convective motions are isolated, fast, filamentary, and twisting downdrafts that merge into successively larger scale downdrafts with depth (Stein & Nordlund, 1989). Such filamentary downdrafts may work to "stiffen" the vertical structure. Only near the boundaries does this mechanism become ineffective and deviations from radial rotation contours can occur.

As long as it is impossible to resolve sufficiently small scales in a global 3-D simulation it may be useful to incorporate a mean-field approach with simulations of the small-scale behavior. The ultimate aim would be to apply the results for the derived mean-field transport coefficients to the computation of such global models. However, there are major problems with this approach. The presence of artificial boundaries, the only slightly turbulent flow, and the relatively short range of different length scales are all unrealistic properties of our simulated flow. It might appear reasonable to identify the computational boundaries with the upper and lower boundaries of the convection zone. This would be, however, incompatible with the idea of examining the turbulent flow only in a small test volume. The present investigations have demonstrated that the test volume concept allowes us to impose systematic gradients. This is important, because plausible results for the turbulent diffusivities were only obtained after imposing such gradients.

Future investigations should be performed also with quite different boundary conditions, because this can give some information about the restrictions imposed by such conditions. It has now become feasible to perform a number of runs with different magnetic field strength (Chandrasekhar number) to see at what parameter values nonlinear effects set in. Similarly a possible saturation for high inverse Rossby numbers might be detected by varying the ratio of Taylor number to Rayleigh number. Investigating the dependence of the α-effect on latitude as well as on the field orientation would provide a further test.

References

Brandenburg, A., Nordlund, Å, Pulkkinen, P., Stein, R. F., Tuominen, I.: 1990, *Astron. Astrophys.* (Paper I, in press)

Krause, F., Rädler, K.-H.: 1980, *Mean-Field Magnetohydrodynamics and Dynamo Theory*, Akademie-Verlag, Berlin

Nordlund, Å., Stein, R.F.: 1989, in *Solar and Stellar Granulation*, eds. R. Rutten and G. Severino, Kluwer Acad. Publ.

Roberts, P. H., Soward, A. M.: 1975, *Astron. Nachr.* **296**, 49

Rüdiger, G.: 1989, *Differential rotation and Stellar Convection: Sun and solar-type stars*, Gordon & Breach, New York

Rüdiger, G., Kichatinov, L. L.: 1990, *Astron. Astrophys.* (in press)

Stein, R.F., Nordlund, Å.: 1989, *Astrophys. J. Letters* **342**, L95